Scaling of radial seals

Matthias Kröger, Robert Teichert, Yongzhen Lin

Standard seals are required in almost all conceivable machine solutions for common nominal diameters. A common practice here is to transfer an initial original design of one diameter to a large number of other diameters. In this way, the seal manufacturers can implement an adapted scaling of the series, which ensures the safe function of the individual size. This work investigates radial shaft seals in three dimensions to check the different designs. Differences in the contact size and the radial load are observed. On the experimental side, oil and grease lubrication has been investigated. For the investigated seal type differences in the friction characteristic are observed.

1 Introduction

Seals are available in various designs and in many sizes adapted to the nominal diameter. In addition, there are many variants for the outer diameter and the width of the seal. Therefore, the standard seals must be designed in many different sizes.

Different scaling methods can be used. On the one hand, the seal lip design can be retained and only the nominal diameter adjusted. On the other hand, the sealing lip could be scaled along with the size and thus the sealing lip could become smaller resp. larger. The radial force plays an important role. The radial force per length could be kept constant as a line load. Further the contact pressure could be hold constant. The contact width and radial force of the tested seals are therefore investigated as tribological relevant parameters.

2 Test configuration

In this work, rotary shaft seals with helical springs are investigated, see Figure 1. These consist of an elastomer base body whose rigidity is increased by a metal ring vulcanised into it. The spring increases the radial force of the seal and can be additionally controlled by this in addition to the geometry of the base body. The seal material is 72 NBR 902 [4]. The seals are further characterised by Table 1. The tests show whether a size influence can be determined.

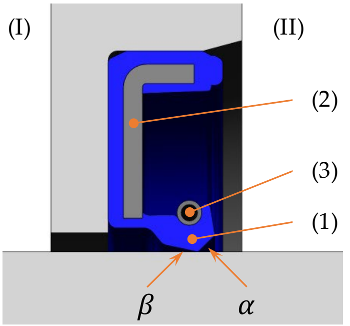

Figure 1: Radial shaft seal with worm spring: (I) Air side/bottom side. (II) Oil side/face side, (1) Sealing lip, (2) Stiffening ring, (3) Worm spring, α Oil side angle, β Air side angle [3].

Table 1: Investigated seals and their characteristics [4].

Seal	Nominal diameter d [mm]	Outer diameter D [mm]	Width B [mm]	Material	Hardness Shore A
A	20	40	6	72 NBR 902	72 ±5
B	45	66	6	72 NBR 902	72 ±5
C	100	100	6	72 NBR 902	72 ±5

2.1 Radial load

The radial force measuring device, see Figure 2, uses the two-jaw measuring method. When the seal is placed there, both half cylindrical jaws are pressed together. The right side is anchored to the frame, while the left side is flexibly mounted via leaf springs and measures the forces via a force sensor. The measured force must be multiplied by π and results in the radial force of the seal.

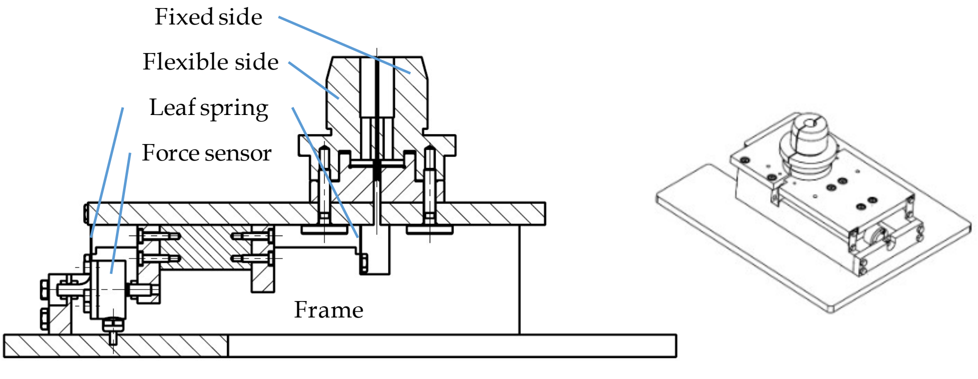

Figure 2: Sketch of the radial force measuring device [3].

The measured radial forces are shown in Table 2. These were investigated with the helical spring and without the helical spring. The mean values from 5 measurements increase degressively with the diameter. The contribution of the helical spring to the radial forces is approx. 25% for the small seal, approx. 35% for the mean sized seal and approx. 50% for the large seal.

Table 2: Measured radial forces F_{Rad} with and without helical spring [3].

Seal	Number of Measurements	Mean value	Variation
		N	%
A	5	17,688	3,80
A, without helical spring	5	13,336	3,91
B	5	25,572	4,45
B, without helical spring	5	16,638	7,12
C	5	32,448	1,92
C, without helical spring	5	16,840	7,29

The line load f is calculated from the radial force F_{Rad} and the circumference πd:

$$f = \frac{F_{Rad}}{\pi d} \tag{1}$$

Values of line load f of 0,28 N/mm, 0,18 N/mm resp. 0,15 N/mm results for the diameters of 20 mm, 45 mm resp. 70 mm with helical spring. The line load is significantly reduced with increasing nominal diameter.

2.2 Contact width

The contact width is measured optically with a digital microscope via a mirror with mirror holder (1), see Figure 3. The seal is pushed onto the top of an transparent tube (2) for this purpose. Illumination with an LED (4) from below makes the contact surface appear bright due to the refractive properties of the light.

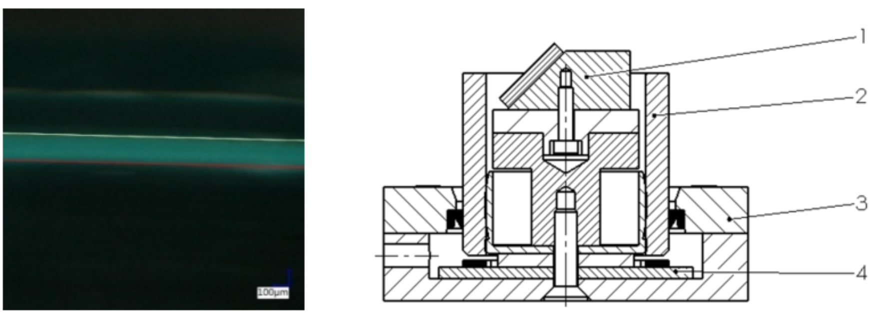

Figure 3: Optical measurement of contact width
1: Mirror with holder, 2: Transparent tube, 3: Housing, 4: Board with LED [3].

The contact widths were measured before the tests (new) and after the tests (used), see Table 3. The contact width of the gasket with 45 mm is significantly smaller than the other two sizes. The seals with 20 mm and 70 mm have very similar contact widths. Due to the circumference, the contact area increases with the diameter. The contact widths after use are about twice the original contact widths.

Table 3: Results of contact width measurements [3].

Seal	Nominal diameter d	Contact width b new	Contact width b used	Contact area A new	Contact area A used
	mm	mm	mm	mm^2	mm^2
A	20	0,098	0,189	6,18	11,88
B	45	0,062	0,135	8,86	19,09
C	70	0,099	0,218	21,84	47,98

An important value for the tribological contact is the contact pressure, which is used e.g. in the Gümbel-diagram [3]. With the radial force F_{Rad} and the original contact area A the contact pressure p is calculated:

$$p = \frac{F_{Rad}}{A} \tag{2}$$

Values of contact pressure p are 2,86 N/mm^2, 2,89 N/mm^2 resp. 1,49 N/mm^2 for the nominal diameters of 20 mm, 45 mm resp. 70 mm with helical spring. Both smaller seals have almost the same contact pressure while the larger seal has approx. half contact pressure.

2.3 Lubrication

As lubricants are used one oil and three greases. The oil is a reference oil according to the specifications of the Forschungsvereinigung Antriebstechnik called FVA 3. Three greases suitable for rolling bearing applications were selected as lubricating greases. The greases BG 1 to BG 3 have very different nominal kinematic viscosities of 400 mm^2/s, 100 mm^2/s and 15 mm^2/s, respectively. The most important data of the lubricants can be found in Table 4.

Table 4: Description of the greases and oil used [3].

Name	Base oil type	Thickener type	Kinematic viscosity ν		Drop point	Walk-penetration	NLGI class
			40 °C mm^2/s	100 °C mm^2/s	°C	0,1 mm	
FVA 3	Mineral	-	95	11	-	-	-
BG 1	Mineral	Lithium-Calcium	400	27	>175	265 - 295	2
BG 2	Mineral	Lithium	100	10	>165	265 - 295	2
BG 3	Mineral/ Synthetic	Lithium	15	3.5	>190	265 - 295	2

2.4 Seal test rig

The radial seal test rig has been built specially for measuring frictional torques and seal temperatures, see Figure 4. It consists of a test head, a bearing unit and a motor. In the test head, the seal is installed in a seal adapter. A ground bearing inner ring serves as contact surface. The seal support is attached to the torsional moment sensor via an insulating body for thermal insulation.

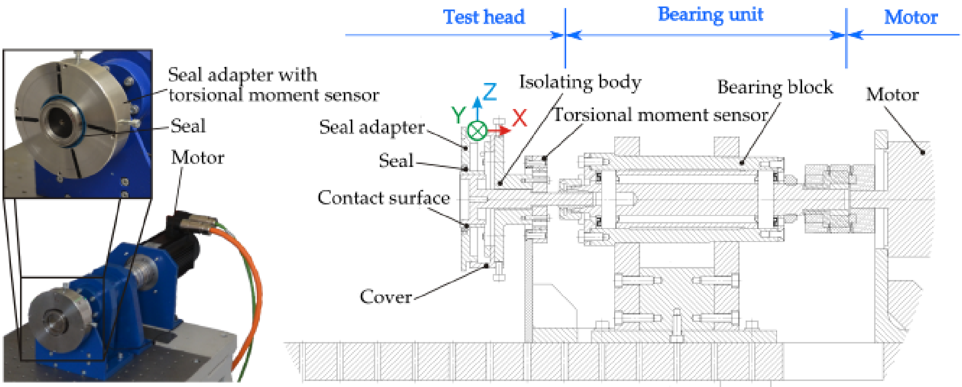

Figure 4: Sketch of radial seal test rig [3].

The shafts have different designs depending on the tested seal diameter, see Figure 5. Bearing inner rings are pressed onto the shafts as counter parts in contact with the seal.

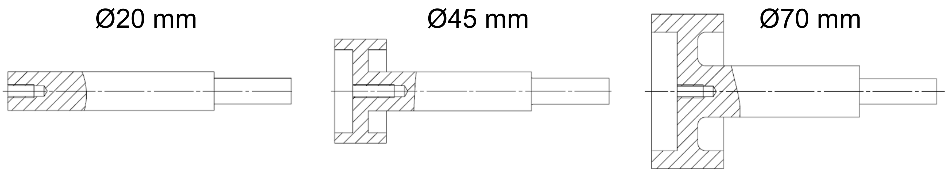

Figure 5: Sketch of the shafts for different seal diameters [3].

2.5 Seal tests

Figure 6 to Figure 8 show the curves of the friction coefficient and the temperature of the sealing lips for the seals with diameter 20 mm, 45 mm and 70 mm. Before the actual main test runs, each seal is preconditioned by a two-hour test run at maximum speed with the FVA 3 oil. The main test is carried out in ascending order of the circumferential speeds to be tested. Every main test is performed three times with three different seal samples with every lubricant by an hour test time for each velocity. The lubricant itself is placed on the shaft before the assembly. For a continuous support the oil lubrication is carried out with a syringe pump, which maintains a minimum lubrication by supplying lubricant at set times. In contrast, a defined quantity of grease is applied to the area of contact between the seal and the shaft during grease lubrication.

All seals initially show an increase in the coefficient of friction at low speeds. At high speeds, the coefficient of friction decreases again. The highest coefficients of friction occur with the high-viscosity grease, the lowest with the low-viscosity grease. The temperatures at the seal increase strongly with the circumferential speed to values around or above 100°C.

For the BG 1 grease, tests were only carried out up to and including a circumferential speed of 2.5 m/s. The reason for this is the excessively high temperature development, which leads to temperatures above 120°C. Above this operating temperature, which is permissible for the material NBR, the rubber dissolves.

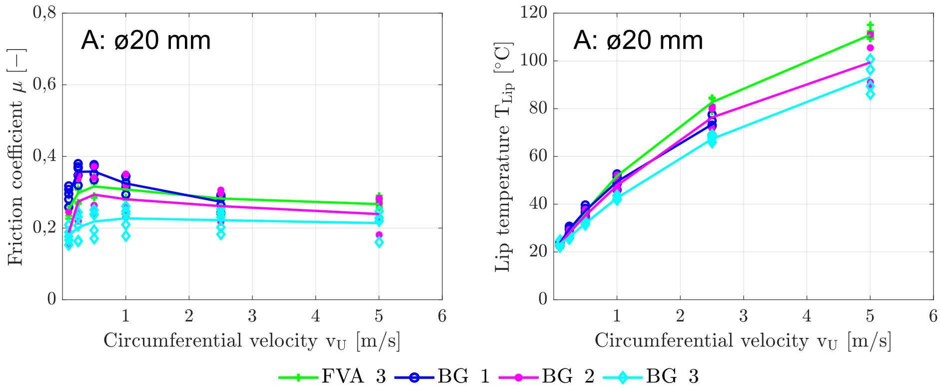

Figure 6: Friction coefficient and temperatures of seal A with 20 mm nominal diameter [3].

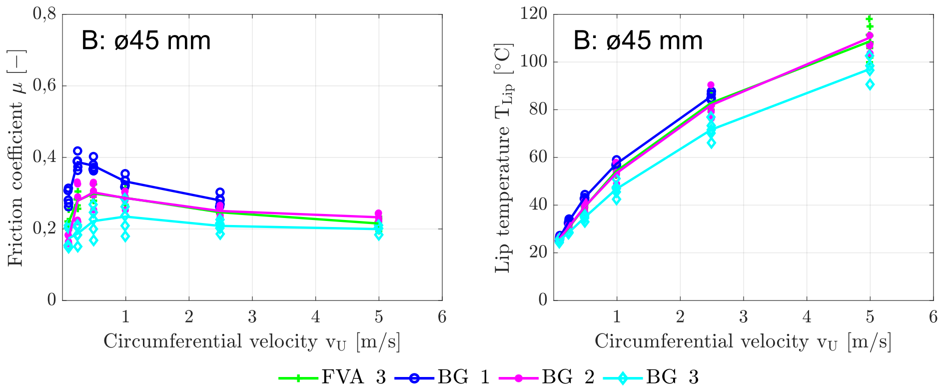

Figure 7: Friction coefficient and temperatures of seal B with 45 mm nominal diameter [3].

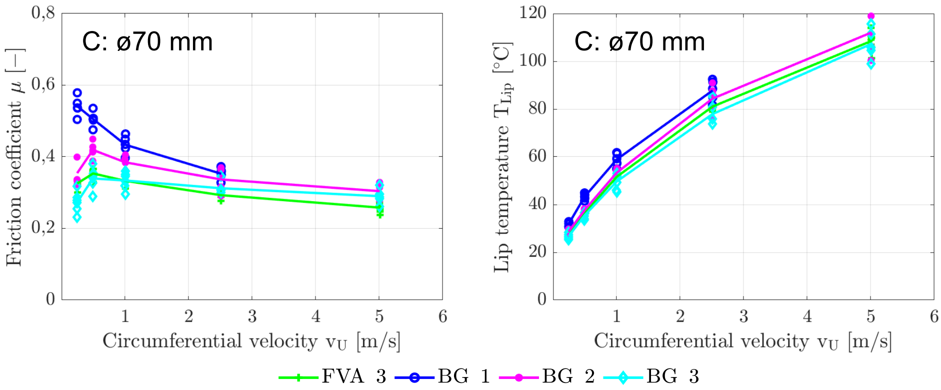

Figure 8: Friction coefficient and temperatures of seal C with 70 mm nominal diameter [3].

A comparison of the seals is shown in Figure 9. The 3 seals show clear differences with regard to the coefficients of friction. The 20 mm and 45 mm seals have significantly lower coefficients of friction than the 70 mm seal. In particular, the high viscosity grease shows significantly higher coefficients of friction with the 70 mm seal.

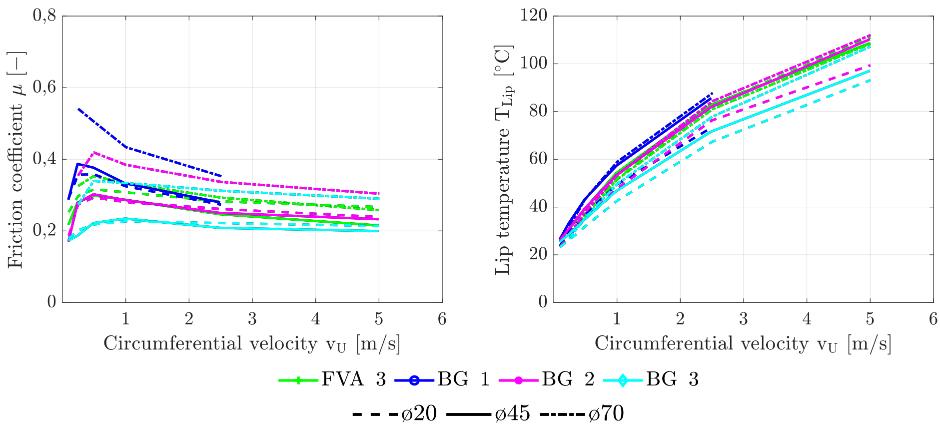

Figure 9: Comparison of the friction values and temperatures of the three seal sizes [3].

The temperature characteristics show similar phenomena for BG1 and BG2. The temperature curve is approximately the same for these, although slightly larger temperatures were measured for the larger diameter. The temperature curve for the nominal diameter 20 mm, on the other hand, is significantly smaller for these. In contrast, a more uniform picture emerges for BG 3, where the temperature values per speed step are more even. The temperatures for the oil lubrication are closely scaled.

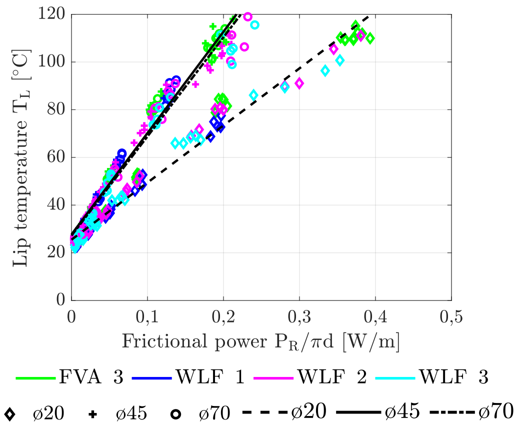

Figure 10: Seal lip temperature for the three seal dimensions:
Lip temperature as function of circumferential frictional power $T_L = f(P_R/\pi d)$ [3].

To illustrate the thermal influence of the test setup, the sealing lip temperatures are plotted as a function of the circumferential frictional power $P_R/\pi d$ according to Feldmeth [2], see Figure 10 with equation (3):

$$\Delta T = K_{D1} \frac{P_R}{\pi d} \tag{3}$$

Here, ΔT indicates the temperature difference to the ambient temperature. Almost identical approximations can be determined for the seals with 45 mm and 70 mm nominal diameters, whereby these represent the measured results well. For the seal with 20 mm nominal diameter, a significantly flatter temperature increase is obtained. This can be explained by the significantly different structure of the shaft, compare Figure 5.

Another functional representation of seal lip temperature is as a function of friction power alone, see equation (4), which is based on Berndt. Reference to the nominal diameter or other seal geometries is not required here.

$$\Delta T = K_{D2} \cdot P_R \tag{4}$$

In analogy to the previous figure, the lip temperature according to this approach is represented in Figure 11. Here, a clear separation of the approximation curves can be seen. These linear functions show the strongest slope for the smallest diameter. With increasing diameter, the slope decreases at the same time.

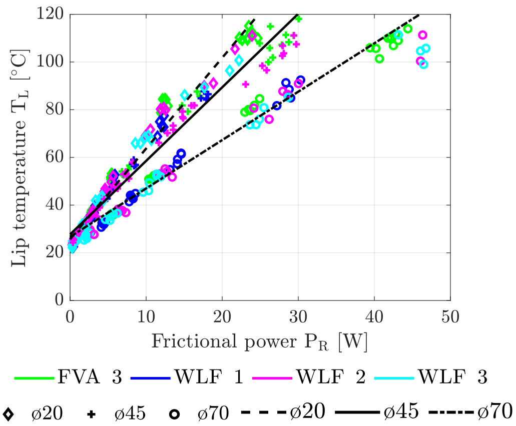

Figure 11: Seal lip temperature for the three seal dimensions: Lip temperature as function of frictional power $T_L = f(P_R)$ [3].

The equation (5) is used to calculate the temperature of the sealing lip:

$$T_{Lip} = T_0 + (m_d \cdot d + K_{D2,0}) \cdot P_R \tag{5}$$

with

$$\mathrm{K}_{D2} = \mathrm{m_d} \cdot \mathrm{d} + \mathrm{K}_{D2,0} \tag{6}$$

A parameter analysis was performed for the parameters introduced in the equation. This can be seen in Figure 12. Based on the behavior of the factor $\mathrm{K}_{D2,0}$, a linear regression is used for its calculation, see equation (6). The zero temperature T_0 is approximately constant over the diameters and is equated with the mean value of the measuring points. The values necessary for the temperature calculation were determined and can be found in Table 5.

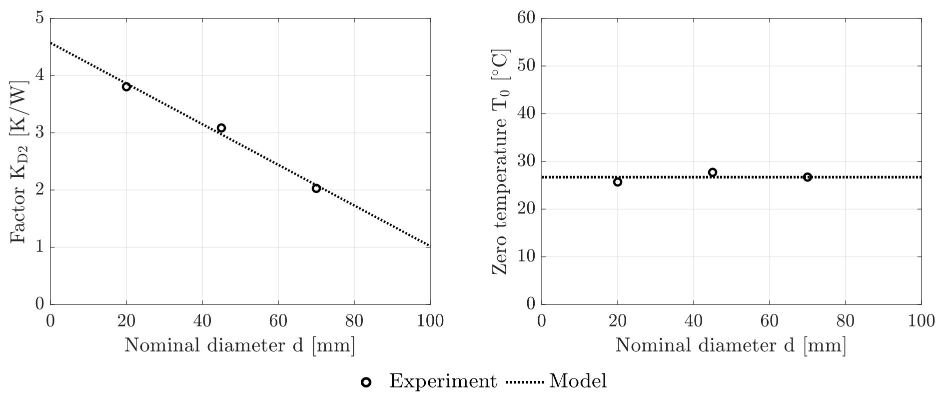

Figure 12: Calculation factors for friction power-related sealing lip temperature as a function of the shaft diameter [3].

Table 5: Calculation parameters for the approximation constant [3].

m_d	$K_{D2,0}$	T_0	
$\left[\frac{K}{W \cdot mm}\right]$	$\left[\frac{K}{W}\right]$	$[°C]$	$[K]$
-0,0355	*4,5707*	*26,70*	*299,85*

The approach was applied in Figure 13 for arbitrary diameters inside and outside the investigated diameter spectrum for both designs. It is clearly visible that for the diameters within the investigated area from 20 mm to 70 mm (shown in red) a good mapping is made possible by the model, the same applies to the range of decreasing diameters. The strong temperature development can be understood by a poorer heat dissipation possibility due to the smaller shaft diameter.

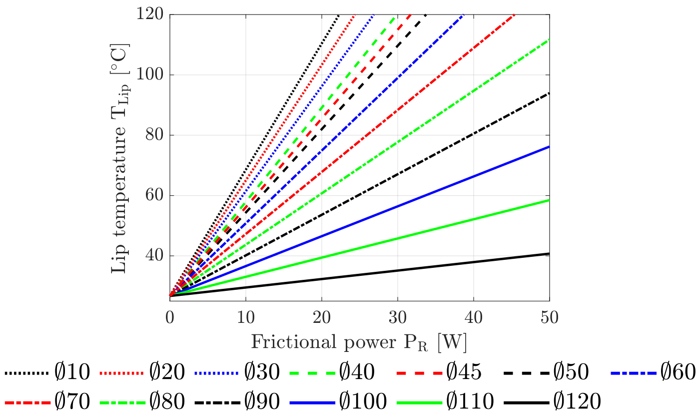

Figure 13: Simulation of the temperature as a function of the diameter with input of the frictional power [3].

On the other hand, the range not shown in the figure above for diameters higher than 120 mm must be critically questioned, since there is a temperature reduction from the beginning with increasing friction power. However, this approach is sufficient for investigations on the radial seal test rig, as it is limited to investigation diameters of a maximum of 100 mm. For further validation of this approach, however, investigations below and above the previous diameter spectrum are useful.

3 Summary and Conclusion

Radial seals with three different nominal diameters were investigated. The results show that the radial force increases degressively with the nominal diameter of the seals investigated. On the other hand, the line load, as force related to the circumference, decreases significantly with the nominal diameter. The contact width in the unused state ranges between 0.06 mm and 0.1 mm for the seals investigated and shows no clear tendency with respect to the seal size. The medium diameter seal has significant smaller contact width. The contact pressure of the largest seal is half of that of the both other seals. The coefficient of friction is significantly higher for the largest seal and the grease with high viscosity than for the other seals and lubrications.

It is obvious that a clear scaling characteristic could not be found for the investigated seals. An additional investigation on seals without worm spring had shown also no clear scaling characteristic [3]. More detailed statement on the scaling characteristic of seals would require even more extensive investigation.

4 Nomenclature

Variable	***Description***	***Unit***
α	Oil side angle	[rad]
A	Contact area	[mm^2]
β	Air side angle	[rad]
B	Width	[mm]
b	Contact width	[mm]
d	Seal nominal diameter	[mm]
D	Seal outer diameter	[mm]
f	Line load	[N/mm]
F_{Rad}	Radial force	[N]
K_{D1}	Temperature factor	[K/W]
K_{D2}	Temperature factor	[K/W]
μ	Friction coefficient	[-]
m_d	Increase for the temperature factor	[K/(W·mm)]
p	Contact pressure	[N/mm^2]
P_R	Frictional power	[W]
T	Temperature	[°C]; [K]
T_0	Zero temperature	[°C]; [K]
T_{Lip}	Lip temperature	[°C]; [K]
v	Kinematic viscosity	[mm^2/s]
v_U	Circumferential velocity	[m/s]

5 References

[1] Berndt, C.: Tribologie von Radial-Wellendichtungen. Dissertation. Books on Demand, Norderstedt, 2019.

[2] Feldmeth, S.; Bauer, F.; Haas, W.: Temperaturbestimmung bei Radial-Wellendichtungen mittels CHT-Simulation: 53. Tribologie-Fachtagung 2012.

[3] Teichert, R.: Tribologie von fettgeschmierten Radialwellendichtungen. Dissertation. (eingereicht)

[4] Freudenberg Sealing Technologies: Technisches Handbuch. https://www.fst.com/-/media/files/fst,-d-,com/technical-manuals/de/fst_technisches_handbuch_2015_kap01_simmerringe_und_rotationsdichtungen.pdf, Stand: 28.01.2021.

6 Authors

University of Technology Bergakademie Freiberg, Institute of Machine Elements, Design and Manufacturing (IMKF)

Agricolastraße 1, 09599 Freiberg, Germany:

Univ.-Prof. Dr.-Ing. Matthias Kröger ORCID 0000-0002-4132-8323, kroeger@imkf.tu-freiberg.de

Robert Teichert, M.Sc., ORCID 0000-0003-3574-4360, robertteichert@gmx.net

Yongzhen Lin, M.Sc., yongzhen.lin@imkf.tu-freiberg.de